Energy Conversion and Management 205 (2020) 112443

Contents lists available at ScienceDirect

Energy Conversion and Management

journal homepage: www.elsevier.com/locate/enconman

An enhanced adaptive differential evolution algorithm for parameter extraction of photovoltaic models

Shuijia Li[a,b], Qiong Gu[a,*], Wenyin Gong[b,*], Bin Ning[a]

[a] School of Computer Engineering, Hubei University of Arts and Science, Xiangyang 441053, China
[b] School of Computer Science, China University of Geosciences, Wuhan 430074, China

ARTICLE INFO

Keywords:
Parameter extraction
Adaptive differential evolution
Photovoltaic models
Optimization algorithm

ABSTRACT

Parameter extraction of photovoltaic models based on measured current-voltage data plays an important role in the simulation, control, and optimization of photovoltaic systems. Although many parameter extraction techniques have been devoted to solving this problem, they may suffer from some deficiencies. In this paper, an enhanced adaptive differential evolution algorithm is proposed to extract photovoltaic parameters fast, accurately and reliably. In proposed method, the crossover rate sorting mechanism is introduced to assign each individual to an adapted crossover rate value according to their fitness values, which allows good elements to be more inherited in next generation. In addition, a dynamic population reduction strategy is used to improve the convergence speed and balance the exploration and exploitation. The performance of proposed method is confirmed by extracting parameters of different photovoltaic models, i.e., single diode, double diode, and photovoltaic modules. The simulated results show that the proposed method exhibits competitive performance on accuracy, reliability and convergence speed compared with other state-of-the-art algorithms. Further, the test results on experimental data from the manufacturers data sheet also indicate that the proposed algorithm can obtain superior solutions at different irradiance and temperature. Therefore, the proposed method can be an effective and efficient alternative for parameter extraction of photovoltaic models.

1. Introduction

To deal with the serious environmental and social problem caused by the widespread use fossil based fuels, renewable energy sources have been focused on great attention recently [1]. There are many alternative renewable energy options to fossil fuels [2], such as solar, geothermal, hydropower, wind, and biomass energy. Among these energy sources, solar energy has attracted great attention [3] due to its promising features like no gas emission, renewability, and freely available. Currently, photovoltaic (PV) systems play a vital role in todays electric power systems [4], because it can directly convert solar energy into electricity [5] as well it is noise-free and easy to install [6]. For a PV system, the choice of PV model is crucial [7], which is used to envisage to imitate the behavior of real PV cells, i.e., fits its measured current–voltage (*I-V*) data under all operating conditions [8]. Although various PV models were proposed, the most commonly used in practice is the single diode model (SDM) and the double diode model (DDM) [9]. For these PV models, it is essential to extract the parameters fast, accurately and reliably. However, the current equation of PV models is an implicit and non-linear equation [10], which results in that it is still an extremely important and challenging work.

In recent years, many optimization algorithms have been employed to extract the parameters of PV models, which can be classified into three different families. The first is based on the analytical approaches that solve the problem by analyzing the mathematical equations, such as analytical extraction method [11] and key points method [12]. Although such methods can obtain results quickly and easily, some assumptions need to be made in advance leading to inaccurate solutions. The second family is deterministic methods, typically the Newton-Raphson method [13] and the Lambert W-functions [14]. This type of method has a strong local search ability, but it is also highly sensitive to the initial solution and easy to trap into local optimal. More importantly, deterministic methods have extremely strict requirements on the objective function equation of the model like differentiability and convexity, while the actual model often fails to meet. The remaining family is the meta-heuristic method that overcomes the shortcomings of the first two families. Due to no strict requirements of the objective function and easy to implement, meta-heuristic methods have been drew growing attention and many researchers have tried to apply them for parameter extraction of PV models. In [15], simulated annealing algorithm was used for PV parameters identification. In [16], genetic

* Corresponding authors.
E-mail addresses: qionggu@hbuas.edu.cn (Q. Gu), wygong@cug.edu.cn (W. Gong).

https://doi.org/10.1016/j.enconman.2019.112443
Received 9 July 2019; Received in revised form 2 December 2019; Accepted 25 December 2019
Available online 07 January 2020
0196-8904/

algorithm was applied for identification of PV solar cells and modules parameters. In [17], an improved particle swarm optimisation with adaptive mutation strategy was proposed for photovoltaic solar cell/module parameter extraction. In [18], the authors proposed a penalty based differential evolution for estimating the parameters of solar PV modules at different environmental conditions. In [19], a repaired adaptive differential evolution was used to the parameter of solar cell models accurately. In [20], an improved JAYA algorithm with a self-adaptive weight was proposed for parameters identification of PV models. In [21], a performance-guided JAYA algorithm was proposed for extracting parameters of different PV models. In [22], multiple learning backtracking search algorithm was developed to accurately and reliably extract the parameters of PV models. In [10], TLBO with a generalized opposition-based learning was used to extract the parameters of solar cell models. In [23], a self-adaptive strategy was introduced into TLBO to improve PV parameter identification problem. In [24], a hybrid teaching-learning-based artificial bee colony was proposed for PV parameter estimation. In [25], an improved teaching and learning strategies with TLBO was used to accurately and reliably extract the parameters of different PV models. The results reported by these meta-heuristic methods are satisfactory, which indicates that meta-heuristic methods are promising alternative for parameter extraction of PV models. However, from Section 5, the algorithm used in the above literature still has room for further improvements in terms of convergence speed and reliability, especially for the DDM.

Differential evolutionary (DE), a stochastic population-based search method, was proposed by Storn and Price in 1997 [26], which has been considered a simple yet efficient numerical optimization algorithm. Due to several promising features like fast convergence, robustness, and good at global search ability, various advanced DE variants have been developed and widely used in various fields [27]. Among all DE variants, JADE [28] is deemed as one of the most successful variants, obtained promising results in the benchmark problems. Nonetheless, JADE still has some shortcomings, for example, the generated crossover rate (*CR*) is randomly assigned to each individual, not taking individual fitness values into account. In addition, the common algorithmic parameter (i.e., population size) is difficult to give immediately for different problems.

In order to make use of the JADE algorithm to solve PV parameter extraction problems quickly, accurately, and reliably, in this paper, an enhanced adaptive differential evolution algorithm, referred as EJADE, is proposed for the shortcomings of JADE mentioned above. In EJADE, the *CR* sorting mechanism is introduced to more rationally assign *CR* values to each individual. To be specific, an individual with better fitness value will be assigned to a smaller *CR* value to allow more good elements to be inherited, while a larger *CR* value will be assigned to an individual with poorer fitness value to accept more mutant elements. In addition, a dynamic population reduction strategy is employed to improve the convergence speed and balance the exploration and exploitation in the process of evolution. To verify the effectiveness of the proposed EJADE algorithm, it is used to extract parameters of different PV models. The simulation and comparison results show that proposed EJADE algorithm outperforms other well-established meta-heuristic algorithms.

The main contributions of this paper are given as follows:

- An enhanced adaptive differential evolution (EJADE) algorithm is proposed to extract parameters of different PV models. In EJADE, the *CR* sorting mechanism is introduced to more rationally assign *CR* values to each individual. In addition, a dynamic population reduction strategy is employed to accelerate convergence and establish a trade-off between the exploitation and exploration.
- The performance of EJADE has been extensively investigated by parameter extraction of different PV models, including two PV modules at different irradiance and temperature.
- An effective method for solving PV model parameter identification problems is provided.

The rest of this paper is arranged as follows. Section 2 gives the statement of SDM, DDM and objective functions. The original JADE algorithm is briefly described in Section 3. Section 4 provides the proposed enhance adaptive differential evolution algorithm in detail. Section 5 carries out the experiments and analyzes the results. Finally, the conclusions are given in Section 6.

2. Problem statement

As mentioned in Section 1, there are two most commonly used models in practice, the single diode model (SDM) and the double diode model (DDM). In this section, the SDM, the DDM, the PV module based the SDM (SMM), and the objective function are described.

2.1. Single diode model

The equivalent circuit of SDM is given in Fig. 1(a), where it can be seen that there is a current source, a diode, and two resistors. The output current I can be formulated as follows [29]:

$$I = I_{ph} - I_d - I_{sh} \tag{1}$$

where I_{ph} is the photo-generated current, I_d and I_{sh} denote the diode current and shunt resistor current, respectively, and they are calculated as below:

$$I_d = I_o\left[\exp\left(\frac{V + IR_s}{aV_t}\right) - 1\right] \tag{2}$$

$$I_{sh} = \frac{V + IR_s}{R_{sh}} \tag{3}$$

where I_o is the diode reverse saturation current, a is the diode ideality factor, R_s and R_{sh} are series and shunt resistance, respectively. V is the cell output voltage, and V_t denotes the junction thermal voltage formulated as follows:

$$V_t = \frac{k \cdot T}{q} \tag{4}$$

where k represents the Boltzmann constant ($1.3806503 \times 10^{-23}$J/K), q denotes the electron charge ($1.60217646 \times 10^{-19}$C), and T is the temperature of junction in Kelvin.

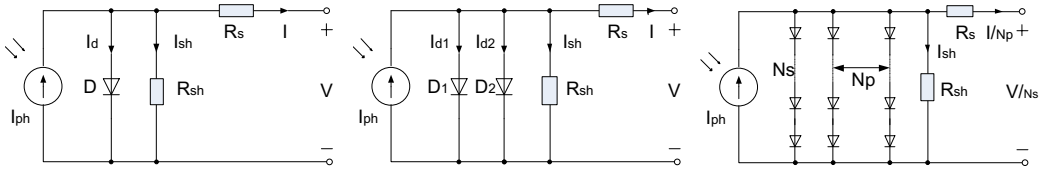

(a) (b) (c)

Fig. 1. Equivalent circuit of PV models: (a) SDM, (b) DDM, (c) SMM.

Combining the above equations, the output current I can be written as Eq. (5), where it can be seen that there are five unknown parameters (I_{ph}, I_o, R_s, R_{sh}, and a) that need to be extracted in SDM.

$$I = I_{ph} - I_o\left[\exp\left(\frac{V + IR_s}{aV_t}\right) - 1\right] - \frac{V + IR_s}{R_{sh}} \tag{5}$$

2.2. Double diode model

As shown in Fig. 1(b), there are two diodes in parallel in the equivalent circuit of DDM. The output current I can be calculated as follows [29]:

$$I = I_{ph} - I_{d_1} - I_{d_2} - I_{sh} \tag{6}$$

where I_{d_1}, I_{d_2} represent respectively the first and second diode currents, which can be expressed as below:

$$I_{d_1} = I_{o_1}\left[\exp\left(\frac{V + IR_s}{a_1V_t}\right) - 1\right] \tag{7}$$

$$I_{d_2} = I_{o_2}\left[\exp\left(\frac{V + IR_s}{a_2V_t}\right) - 1\right] \tag{8}$$

where I_{o_1}, I_{o_2} are diffusion current and saturation current, respectively. a_1, a_2 denote the first and second diode ideality factors, respectively.

Similar to SDM, the output current I of DDM can be expressed as Eq. (9), where seven unknown parameters, including I_{ph}, I_{o_1}, I_{o_2}, R_s, R_{sh}, a_1, and a_2 need to be extracted.

$$I = I_{ph} - I_{o_1}\left[\exp\left(\frac{V + IR_s}{a_1V_t}\right) - 1\right] - I_{o_2}\left[\exp\left(\frac{V + IR_s}{a_2V_t}\right) - 1\right] - \frac{V + IR_s}{R_{sh}} \tag{9}$$

2.3. Photovoltaic module

For the PV module based the SDM (SMM), usually by multiple diodes connected in series or in parallel shown as Fig. 1(c), its relationship of current and voltage is formulated as follows [25]:

$$I = I_{ph}N_p - I_oN_p\left[\exp\left(\frac{V + IR_sN_s/N_p}{aN_sV_t}\right) - 1\right] - \frac{V + IR_sN_s/N_p}{R_{sh}N_s/N_p} \tag{10}$$

where N_s and N_p are the number of solar cells connected in series or in parallel, respectively. Because the SMM adopted in this study are all in series, N_p is set to be 1. Thus, Eq. (10) can be written as follow:

$$I = I_{ph} - I_o\left[\exp\left(\frac{V + IR_sN_s}{aN_sV_t}\right) - 1\right] - \frac{V + IR_sN_s}{R_{sh}N_s} \tag{11}$$

For the SMM, there are also five unknown parameters (I_{ph}, I_o, R_s, R_{sh}, and a) that need to be extracted.

2.4. Objective function

In general, parameter extraction problems are usually transformed into a class of optimization problem to take advantage of optimization algorithms. Similar to [20], the root mean square error (RMSE) is also used as the objective function in this study, which is defined as follows:

$$\mathrm{RMSE}(\mathbf{x}) = \sqrt{\frac{1}{N}\sum_{k=1}^{N} f(V_k, I_k, \mathbf{x})^2} \tag{12}$$

where N is the number of measured I-V data, and $\mathbf{x}$ is a vector that concludes the unknown parameters to be extracted. Therefore, for different PV models, their objective functions can be represented as follow:

- For SDM:

$$\begin{cases} f(V, I, \mathbf{x}) = I_{ph} - I_o\left[\exp\left(\frac{V + IR_s}{aV_t}\right) - 1\right] - \frac{V + IR_s}{R_{sh}} - I \\ \mathbf{x} = \{I_{ph}, I_o, R_s, R_{sh}, a\} \end{cases} \tag{13}$$

- For DDM:

$$\begin{cases} f(V, I, \mathbf{x}) = I_{ph} - I_{o_1}\left[\exp\left(\frac{V + IR_s}{a_1V_t}\right) - 1\right] - I_{o_2}\left[\exp\left(\frac{V + IR_s}{a_2V_t}\right) - 1\right] - \frac{V + IR_s}{R_{sh}} - I \\ \mathbf{x} = \{I_{ph}, I_{o_1}, I_{o_2}, R_s, R_{sh}, a_1, a_2\} \end{cases} \tag{14}$$

- For SMM:

$$\begin{cases} f(V, I, \mathbf{x}) = I_{ph} - I_o\left[\exp\left(\frac{V + IR_sN_s}{aN_sV_t}\right) - 1\right] - \frac{V + IR_sN_s}{R_{sh}N_s} - I \\ \mathbf{x} = \{I_{ph}, I_o, R_s, R_{sh}, a\} \end{cases} \tag{15}$$

3. Adaptive differential evolution

Due to the new mutation strategy and parameter adaptive manner, an adaptive differential evolution, namely JADE [28], is considered as a very effective optimization algorithm in the DE family and has gained wide attention. Similar to DE, JADE also uses four operations, including initialization, mutation, crossover, and selection to solve numerical optimization problems, which will be described briefly in this section.

3.1. Initialization

Generally, there is μ individuals in a population $\mathbb{P}$ and each individual is envisaged as a solution vector consisting of D decision variables. At initialization operation, all individuals are randomly initialized within the specified range. For example, The j-th decision variable of the i-th individual is initialized as follows:

$$x_{i,j} = LB_j + rand\cdot(UB_j - LB_j) \tag{16}$$

where $\mathbf{x}_i$ is the i-th individual. $i = 1, \cdots, \mu$, $j = 1, \cdots, D$. $rand$ is a random number in interval [0,1]. LB_j, UB_j are the lower and upper bound of the j-th dimension, respectively.

3.2. Mutation

In JADE, a new mutation strategy, namely "DE/current-to-$p$best", is proposed to produce the mutant vector, where convergence and reliability performance are taken into consideration. The i-th mutant vector $\mathbf{v}_i$ is generated as follows:

$$\mathbf{v}_i = \mathbf{x}_i + F_i\cdot(\mathbf{x}_{pbest} - \mathbf{x}_i) + F_i\cdot(\mathbf{x}_{r_1} - \mathbf{x}_{r_2}) \tag{17}$$

where $\mathbf{x}_{pbest}$ is randomly produced from the top 100p% individuals in the current population $\mathbb{P}$ and $p \in (0, 1]$. Both r_1 and r_2 are random integer in $\{1, \cdots, \mu\}$ and $r_1 \neq r_2 \neq i$. Note that $\mathbf{x}_{r_2}$ is chosen from the union $\mathbb{P} \cup \mathbb{A}$, of the current population ($\mathbb{P}$) and archived inferior solutions ($\mathbb{A}$) [28]. F_i is the scale factor of $\mathbf{x}_i$, which is generated in the following manner:

$$F_i = randc(\mu_F, 0.1) \tag{18}$$

where $randc$ denotes the Cauchy distribution; F_i is truncated to be 1 if

$F_i > 1$ or regenerated if $F_i \leqslant 0$;μ_F is initialized to be 0.5 and updated by using Eqs. (19) and (20),

$$\mu_F = (1 - c)\cdot\mu_F + c\cdot mean_L(S_F) \tag{19}$$

$$mean_L(S_F) = \frac{\sum_{i=1}^{|S_F|} F_i^2}{\sum_{i=1}^{|S_F|} F_i} \tag{20}$$

where c is a constant in interval (0, 1), and S_F represents the set of all successful mutation factors F_i at each generation.

3.3. Crossover

To maintain the population diversity, the crossover operation is employed to produce trial vectors after mutation. In JADE, the i-th trial vector $\mathbf{u}_i$ is generated as follows:

$$u_{i,j} = \begin{cases} v_{i,j}, & \text{if } rand \leqslant CR_i \,||\, j == jrand \\ x_{i,j}, & \text{otherwise} \end{cases} \tag{21}$$

where $jrand$ is an integer randomly selected from set $\{1, \cdots, D\}$, which ensures that at least one dimension comes from the mutation vector $\mathbf{v}_i$. CR_i denotes the crossover rate of $\mathbf{x}_i$, which is independently generated according to a normal distribution of mean μ_{CR} and standard deviation 0.1 as below:

$$CR_i = randn(\mu_{CR}, 0.1) \tag{22}$$

where CR_i is truncated to [0, 1]. μ_{CR} is initialized to be 0.5 and updated using Eq. (23) after the end of each generation,

$$\mu_{CR} = (1 - c)\cdot\mu_{CR} + c\cdot mean_A(S_{CR}) \tag{23}$$

where $mean_A$ represents the arithmetic mean, and S_{CR} is the set of all successful CR_i at each generation.

3.4. Selection

After mutation and crossover operations, JADE adopts the greedy selection strategy to determine whether the trial vector or the target vector will survive in the next generation, which can be expressed as follow:

$$\mathbf{x}_i = \begin{cases} \mathbf{u}_i, & \text{if } f(\mathbf{u}_i) \leqslant f(\mathbf{x}_i) \\ \mathbf{x}_i, & \text{otherwise} \end{cases} \tag{24}$$

4. Enhanced adaptive differential evolution

In order to fast, accurately, and reliably extract parameters of different PV models, an enhanced adaptive differential evolution, referred to as EJADE, is developed in this section. The motivations for improvement and the improvements are described below.

4.1. Motivations

In DE family, crossover operation plays a vital role in maintaining the current population diversity. Generally speaking, the offspring individuals should inherit more elements from their parent when the parent individuals is close to the optimum; while when the parent individuals are far away from the optimum, the offspring individuals should accept more elements from mutant vectors [30]. To be specific, the individuals with better fitness values should be assigned relatively small CR values while slightly larger CR values are assigned to the individuals with poor fitness values. Simply put, CR values are related to the individual fitness values. However, in JADE, the CR values are randomly assigned to each individual, ignoring its relationship with the individual fitness values. In addition, the size of the population plays an important role in controlling the convergence speed. Small population size results in faster convergence, increasing the risk of converging to a local optimum; while large population size improves the exploration ability, slowing down the convergence speed [31]. With these into consideration, an enhance JADE algorithm (EJADE) is proposed. In EJADE, two improvements are implemented, i.e., CR sorting mechanism and dynamic population reduction strategy, which are described in detail in the following subsection.

4.2. Crossover rate sorting mechanism

In order to establish the relationship between CR and the individual fitness values, the CR sorting mechanism [32] is introduced. First of all, the CR values generated by Eq. (22) are sorted in ascending order shown as follow.

$$CR' = sort(CR, 'ascend') \tag{25}$$

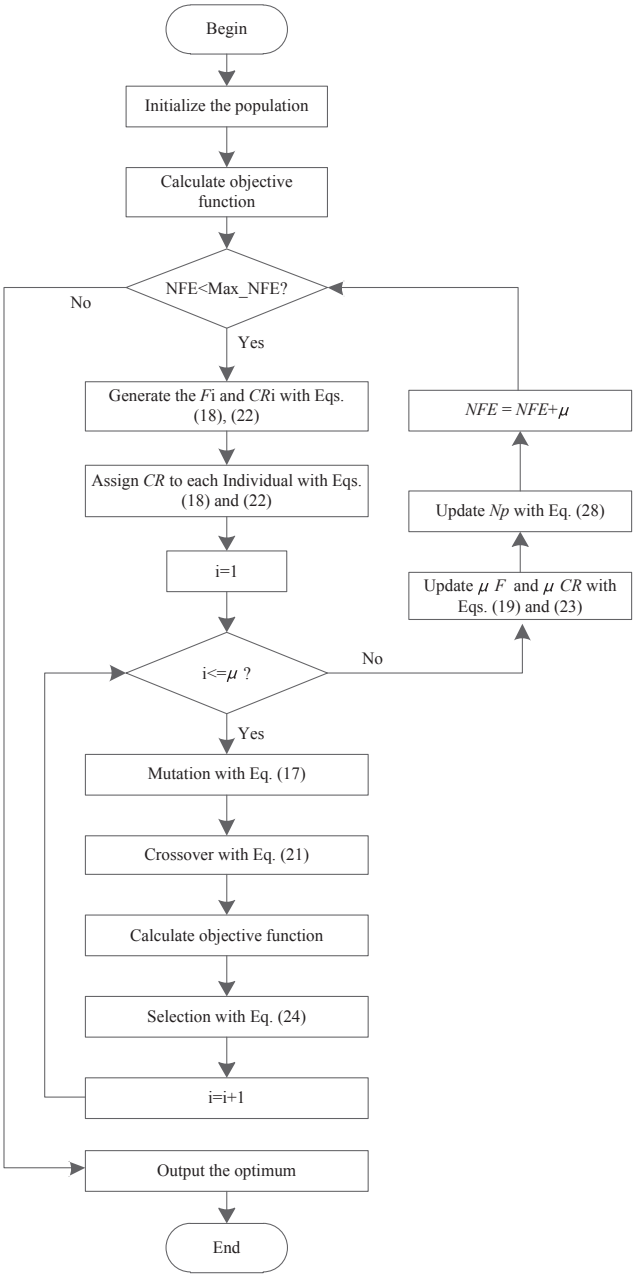

Fig. 2. The flow diagram of EJADE.

Then, individual fitness values are sorted in ascending order to obtain the *index* of each individual as shown in Eq. (26).

$$index = sort(f, 'ascend') \tag{26}$$

Finally, according to the individual fitness values, assign the sorted *CR* values to each individual by using Eq. (27).

$$CR' \rightarrow \mathbf{x}(index) \tag{27}$$

With the *CR* sorting mechanism, the issue that neglecting the relationship between *CR* values and the individual fitness values in JADE can be effectively alleviated.

4.3. Dynamic population reduction strategy

In JADE, the population size μ is a constant throughout the evolution process, which has a great impact on the performance of JADE for solving different optimization problems. In other words, it is not trivial to immediately provide a suitable μ for different problems. To circumvent this issue, a dynamic population reduction strategy is employed to make a good trade-off between the exploitation and the exploration, enhancing the convergence rate of the algorithm. Assume that the current population size is μ_g, the next generation population size μ_{g+1} can be formulated as follows:

$$\mu_{g+1} = floor\left[\left(\frac{\mu_{min} - \mu_{max}}{Max\_NFE}\right) \cdot NFE + \mu_{max}\right] \tag{28}$$

where μ_{min}, μ_{max} are the smallest and the largest population size, respectively. μ_{max} is set to 50, and μ_{min} is set to 4 due to the "DE/current-to-*p*best" strategy in this study. *NFE* represents the number of current function evaluation, and *Max_NFE* denotes the maximum *NFE*. It is noteworthy that whenever $\mu_{g+1} < \mu_g$, the $(\mu_g - \mu_{g+1})$ individuals with poorer fitness values will be eliminated from the current population.

With a dynamic population reduction strategy, a large population size can use the exploration ability to encourage broader exploration of the search space at the early stage. While at the later stage, a small population size does well in exploitation, leading to fast convergence. In this way, the exploitation and exploration capabilities of the algorithm is balanced, and its convergence is also improved.

4.4. Implementation of enhanced adaptive differential evolution

Combining the *CR* sorting mechanism and dynamic population reduction strategy into JADE, an enhanced JADE algorithm, namely EJADE, is implemented. The pseudo code of EJADE is given in Algorithm 1, where it can be seen that EJADE is very simple and easy to implement. Additionally, it does not introduce any additional algorithm parameters other than the inevitable input parameter *Max_NFE*. Note that the *CR* sorting mechanism and dynamic population reduction strategy are used in lines 8 and 16, respectively. Besides the pseudo code of EJADE, Fig. 2 provides the flow diagram of EJADE.

Algorithm 1: The pseudo-code of EJADE

Input: Control parameters: Max_NFE
Output: The optimal solution
1 Set $NFE = 0, \mathbb{A} = [], \mu_{min} = 4, \mu = \mu_{max} = 50$;
2 Initialize the population $\mathbb{P}$ randomly and calculate objective function;
3 $NFE = NFE + \mu$;
4 **while** $NFE < Max\_NFE$ **do**
5 $S_F = []; S_{CR} = []$;
6 **for** $i = 1$ *to* μ **do**
7 Generate the F_i and CR_i using Eqs. (18) and (22) respectively;
8 Assign *CR* to each individual with Eqs. (25), (26), (27);
9 **for** $i = 1$ *to* μ **do**
10 Mutation with Eq. (17);
11 Crossover with Eq. (21);
12 Calculate objective function;
13 Selection with Eq. (24);
14 $NFE = NFE + \mu$, and update $\mathbb{A}$;
15 Update μ_F, μ_{CR} with Eqs. (19) and (23) respectively;
16 Update μ with Eq. (28);

5. Results and analysis

In order to evaluate the performance of proposed EJADE, it is used to extract parameters of different PV models, i.e., SDM, DDM, and SMM. The *I-V* data of SDM and DDM is obtained from [13], which is measured on a 57 mm diameter commercial silicon R.T.C France solar sell under 1000 W/m^2 at 33 °C. The SMM consists of three PV module models, including Photowatt-PWP201, mono-crystalline STM6-40/36 and ploy-crystalline STP6-120/36. The data of Photowatt-PWP201 module measured under 1000 W/m^2 at 45 °C, is obtained from [13]. While the data of mono-crystalline STM6-40/36 obtained from [33] and ploy-crystalline STP6-120/36 obtained from [34], are measured at 51°C and 55 °C, respectively. These PV module models have 36 cells connected in series. Table 1 provides the ranges for each parameter of PV models, which is kept the same as used in previous literatures [10].

For the input parameter of JADE and EJADE, *Max_NFE* is set to be 10, 000 for the SDM and Photowatt-PWP201 module. *Max_NFE* is 20,000 for DDM, while for STM6-40/36 and STP6-120/36 modules *Max_NFE* is 15,000. It is worth mentioning that practical experiments are not carried out due to the expensive equipment. Instead, the

Table 1
Ranges of each parameter.

Parameter	SDM/DDM		Photowatt-PWP201		STM6-40/36		STP6-120/36	
	LB	UB	LB	UB	LB	UB	LB	UB
I_{ph} (A)	0	1	0	2	0	2	0	8
I_o, I_{o1}, I_{o2} (μA)	0	1	0	50	0	50	0	50
R_s (Ω)	0	0.5	0	2	0	0.36	0	0.36
R_{sh} (Ω)	0	100	0	2000	0	1000	0	1500
a, a_1, a_2	1	2	1	50	1	60	1	50

Table 2
Parameter setting of compared algorithms.

Algorithm	Parameter setting
IJAYA	$\mu = 20$
PGJAYA	$\mu = 20$
MLBSA	$\mu = 50$
SATLBO	$\mu = 40$
GOTLBO	$\mu = 50$, *Jumping rate* $J_r = 0.3$
TLABC	$\mu = 50$, *limit* $= 200$, $F = rand(0, 1)$
ITLBO	$\mu = 50$
JADE	$\mu = 50$
EJADE	$\mu_{max} = 50$, $\mu_{min} = 4$

Matlab2016b software is employed to simulate the algorithm and the PV data is substituted into the algorithm to obtain the parameters to be extracted. Note that each algorithm is executed over 30 independent runs and all subsequent experiments are executed on a desktop PC with an Intel Core i5-4590 M processor @ 3.30 GHz, 8 GB RAM, under the Windows 7 64-bit OS.

In addition, to confirm the superior performance of EJADE, seven state-of-the-art algorithms, including IJAYA [20], PGJAYA [21], MLBSA [22], SATLBO [23], GOTLBO [10], TLABC [24], and ITLBO [25] are selected to compare. The parameter settings of the compared algorithms are provided in Table 2. Note that for SDM, DDM and Photowatt-PWP201 module, the results of these comparison algorithms are obtained from corresponding references. While for mono-crystalline STM6-40/36 and ploy-crystalline STP6-120/36 modules, the results are obtained from [25].

5.1. Results on single diode model

For the SDM, the RMSE values and the corresponding extracted parameter values are given in Table 3, where the best results have been marked in **boldface** only when RMSE and NFE are both minimal. From Table 3, it can be observed that EJADE, ITLBO, TLABC, SATLBO, MLBSA, and PGJAYA obtained the best RMSE value (**9.8602E−04**), followed by IJAYA (9.8603E−03), JADE (9.8606E−04), and GOTLBO (9.8744E−04). Although the RMSE value obtained by EJADE is only a little smaller than those algorithms (i.e., IJAYA, JADE, GOTLBO), it is very meaningful for any reduction in the objective function due to the no information available about the accurate values of the parameters. Besides, with the computing resources consumed into consideration, it is evident that EJADE consumed the fewest NFE (**10, 000**) to achieve the best results while ITLBO, TLABC, SATLBO, MLBSA, and PGJAYA consumed a lots of function evaluations (50,000).

In addition, the extracted parameter values of EJADE were used to reconstruct the simulated *I-V* data, whose *I-V* characteristic curve was figured and compared with the measured data as shown in Fig. 3(a). The *I-V* curves clearly indicated that the simulated data are highly coincide with the measured data, which also indirectly manifested that the parameters extracted by EJADE are very accurate.

5.2. Results on double diode model

As mention in subSection 2.2, there are seven unknown parameters that need to be extracted in DDM, which increases the difficulty of parameter extraction problems. In this subsection, EJADE is applied for DDM. The results are given in Table 4, where eight parameter extraction algorithms used in SDM are used to compare. From Table 4, it is obvious that only EJADE and ITLBO achieved the best RMSE value (**9.8248E−04**), while EJADE only consumed **20, 000**, but 50, 000 for ITLBO. It is worth mentioning that TLABC, SATLBO, MLBSA, and PGJAYA that achieved the best results in SDM, do not get the best RMSE value in DDM. In addition, to verify the accuracy of parameter values extracted by EJADE like SDM, the *I-V* curves between measured and simulated data are provided in Fig. 3(b), where the simulated data are also highly consistent with the measured data.

5.3. Results on photovoltaic module model

For the SMM, the experimental results are reported in Tables 5–7. For the Photowatt-PWP201 module, it is clear that all algorithms can achieve the same RMSE value (**2.4251E−03**) while only EJADE and JADE used the least computing resources (NFE = **10,000**). For the results of STM6-40/36 and STP6-120/36 modules, they have a similar point that all algorithms can achieve the same RMSE values (i.e., **1.7298E−03** and **1.6601E−02**), except IJAYA and JADE. However, integrated the RMSE and NFE considerations, only EJADE has achieved

Table 3
Comparison of EJADE with other algorithms on SDM.

Algorithm	I_{ph} (A)	I_o (μA)	R_s (Ω)	R_{sh} (Ω)	a	RMSE	NFE
IJAYA	0.7608	0.3228	0.0364	53.7595	1.4811	9.8603E−03	50000
PGJAYA	0.7608	0.3230	0.0364	53.7185	1.4812	9.8602E−04	50000
MLBSA	0.7608	0.3230	0.0364	53.7185	1.4812	9.8602E−04	50000
SATLBO	0.7608	0.3232	0.0364	53.7256	1.4812	9.8602E−04	50000
GOTLBO	0.7608	0.3316	0.0363	54.1154	1.4838	9.8744E−04	10000
TLABC	0.7608	0.0323	0.0364	53.7164	1.4812	9.8602E−04	50000
ITLBO	0.7608	0.3230	0.0364	53.7185	1.4812	9.8602E−04	50000
JADE	0.7608	0.3229	0.0364	53.6477	1.4811	9.8606E−04	10000
EJADE	0.7608	0.3230	0.0364	53.7185	1.4812	**9. 8602E − 04**	**10000**

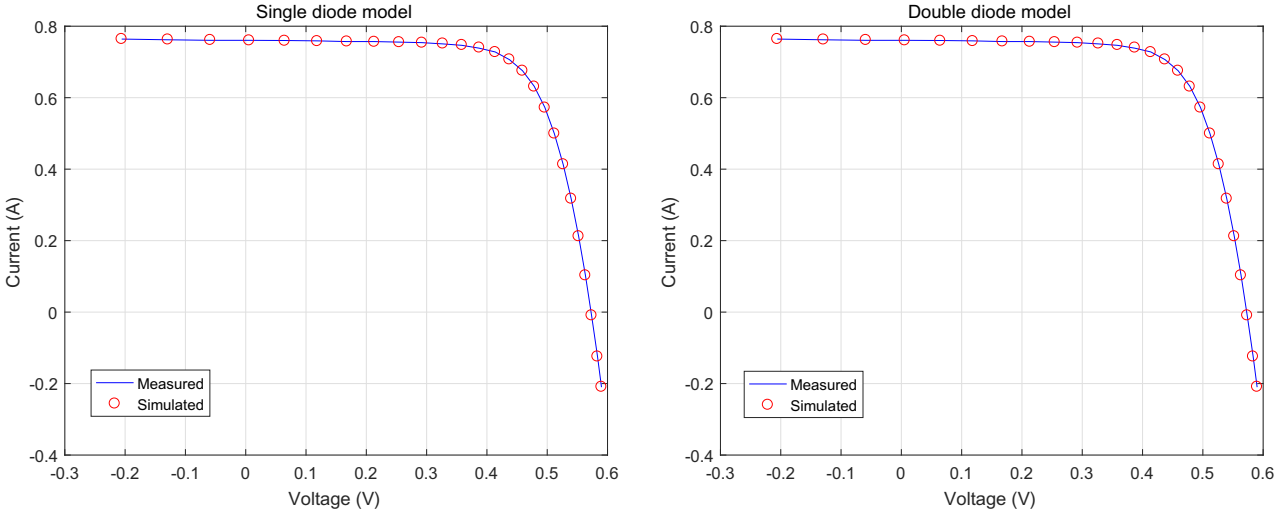

(a) (b)

Fig. 3. Comparison between the measured and simulated data obtained by EJADE: (a) SDM, (b) DDM.

Table 4
Comparison of EJADE with other algorithms on DDM.

Algorithm	I_{ph} (A)	I_{o_1} (μA)	R_s (Ω)	R_{sh} (Ω)	a_1	I_{o_2} (μA)	a_2	RMSE	NFE
IJAYA	0.7601	0.0050	0.0376	77.8519	1.2186	0.7509	1.6247	9.8293E−04	50000
PGJAYA	0.7608	0.2103	0.0368	55.8135	1.4450	0.8853	2.0000	9.8263E−04	50000
MLBSA	0.7608	0.2273	0.0367	55.4612	1.4515	0.7384	2.0000	9.8249E−04	50000
SATLBO	0.7608	0.2509	0.0366	55.1170	1.4598	0.5454	1.9994	9.8280E−04	50000
GOTLBO	0.7608	0.8002	0.0368	56.0753	2.0000	0.2205	1.4490	9.8318E−04	20000
TLABC	0.7608	0.4239	0.0367	54.6680	1.9075	0.2401	1.4567	9.8415E−04	50000
ITLBO	0.7608	0.2260	0.0367	55.4854	1.4510	0.7493	2.0000	9.8248E−04	50000
JADE	0.7608	0.3618	0.0366	54.4683	1.9998	0.2731	1.4669	9.8351E−04	20000
EJADE	0.7608	0.2260	0.0367	55.4854	1.4510	0.7493	2.0000	**9.8248E−04**	**20000**

Table 5
Comparison of EJADE with other algorithms on Photowatt-PWP201.

Algorithm	I_{ph} (A)	I_o (μA)	R_s (Ω)	R_{sh} (Ω)	a	RMSE	NFE
IJAYA	1.0305	3.4703	1.2016	977.3752	48.6298	2.4251E−03	50000
PGJAYA	1.0305	3.4818	1.2013	981.8545	48.6424	2.4251E−03	50000
MLBSA	1.0305	3.4823	1.2013	981.9823	48.6428	2.4251E−03	50000
SATLBO	1.0305	3.4827	1.2013	982.4038	48.6433	2.4251E−03	50000
GOTLBO	1.0305	3.4991	1.2008	989.6889	48.6611	2.4251E−03	50000
TLABC	1.0306	3.4715	1.2017	972.9357	48.6313	2.4251E−03	50000
ITLBO	1.0305	3.4823	1.2013	981.9823	48.6428	2.4251E−03	50000
JADE	1.0305	3.4831	1.2012	982.3236	48.6438	**2.4251E−03**	**10000**
EJADE	1.0305	3.4823	1.2013	981.9824	48.6428	**2.4251E−03**	**10000**

Table 6
Comparison of EJADE with other algorithms on STM6-40/36.

Algorithm	I_{ph} (A)	I_o (μA)	R_s (Ω)	R_{sh} (Ω)	a	RMSE	NFE
IJAYA	1.6637	1.8353	0.0040	15.9449	1.5263	1.7548E−03	50000
PGJAYA	1.6639	1.7389	0.0043	15.9290	1.5203	1.7298E−03	50000
MLBSA	1.6639	1.7387	0.0043	15.9283	1.5203	1.7298E−03	50000
SATLBO	1.6639	1.7387	0.0043	15.9283	1.5203	1.7298E−03	50000
GOTLBO	1.6639	1.7387	0.0043	15.9283	1.5203	1.7298E−03	50000
TLABC	1.6639	1.7387	0.0043	15.9283	1.5203	1.7298E−03	50000
ITLBO	1.6639	1.7387	0.0043	15.9283	1.5203	1.7298E−03	50000
JADE	1.6638	1.7946	0.0042	16.0190	1.5238	1.7324E−03	15000
EJADE	1.6639	1.7387	0.0043	15.9283	1.5203	**1.7298E−03**	**15000**

Table 7
Comparison of EJADE with other algorithms on STP6-120/36.

Algorithm	I_{ph} (A)	I_o (μA)	R_s (Ω)	R_{sh} (Ω)	a	RMSE	NFE
IJAYA	7.4672	2.2536	0.0046	27.5925	1.2571	1.6731E−02	50000
PGJAYA	7.4725	0.0000	0.0046	22.2184	1.2601	1.6601E−02	50000
MLBSA	7.4725	2.3350	0.0046	22.2199	1.2601	1.6601E−02	50000
SATLBO	7.4725	2.3350	0.0046	22.2199	1.2601	1.6601E−02	50000
GOTLBO	7.4725	2.3350	0.0046	22.2199	1.2601	1.6601E−02	50000
TLABC	7.4725	2.3349	0.0046	22.2117	1.2601	1.6601E−02	50000
ITLBO	7.4725	2.3350	0.0046	22.2199	1.2601	1.6601E−02	50000
JADE	7.4645	3.4139	0.0044	1439.6969	1.2926	1.7430E−02	15000
EJADE	7.4725	2.3350	0.0046	22.2199	1.2601	**1.6601E−02**	**15000**

the best results. Moreover, according to the curves fitting results as shown in Fig. 4, where it can be seen that no matter which models, the simulated data of EJADE agreed well with the measured data.

5.4. Statistical results and convergence speed

In the previous sections, the superior accuracy and computational efficiency of proposed EJADE algorithm has been proved by comparing with eight state-of-the-art algorithms. To further verify the reliability of EJADE, the statistical results including minimum (Min), maximum (Max), average value (Mean), standard deviation (Std) and total CPU time for 30 independent runs, are conducted analysis. The statistical results are reported in Table 8, where the following conclusions can be made.

- With respect to the Min RMSE values, many algorithms can provide the best RMSE values for SDM, STM6-40/36 and STP6-120/36 modules. All algorithms obtain the Min RMSE for Photowatt-

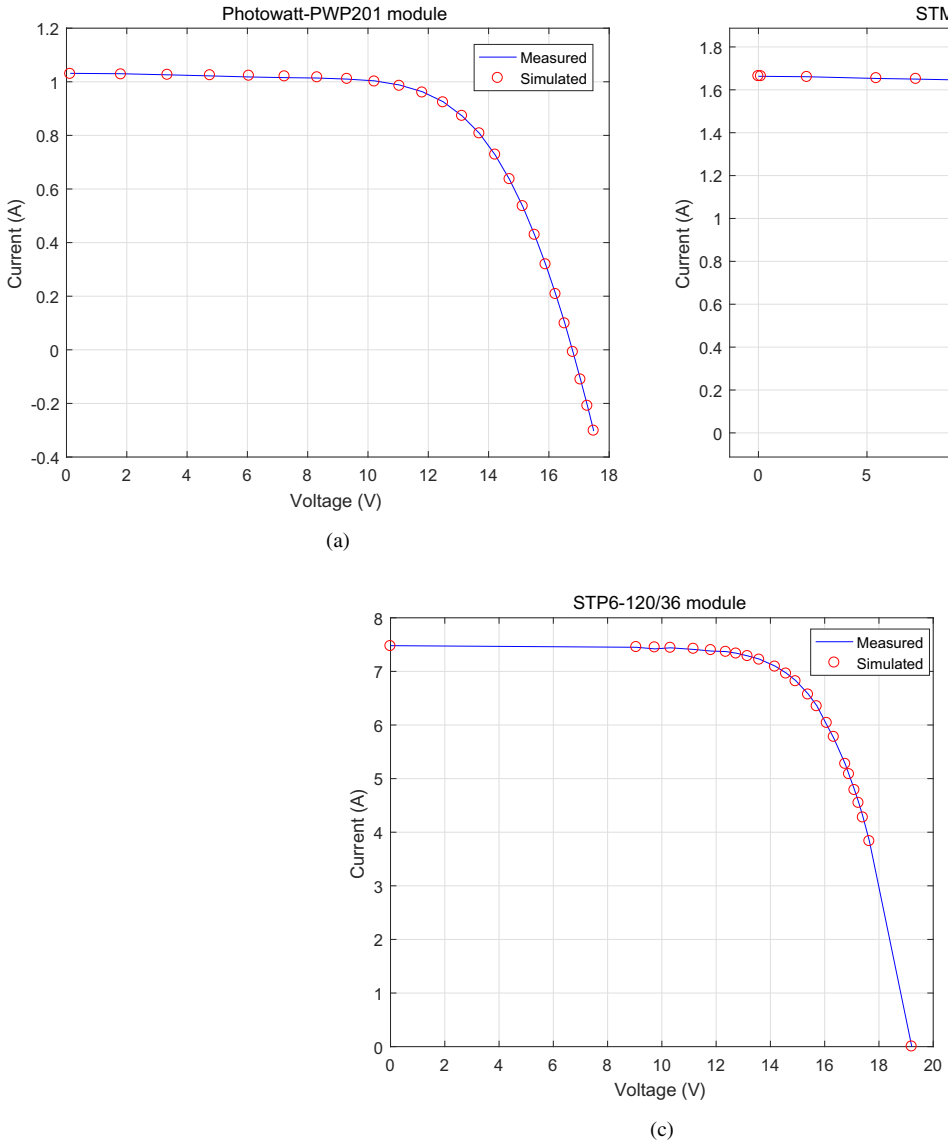

Fig. 4. Comparison between the measured and simulated data obtained by EJADE: (a) Photowatt-PWP201, (b) STM6-40/36, (c) STP6-120/36.

Table 8
The statistical results of SDM, DDM, and SMM.

Model	Algorithm	RMSE				CPU time (s)
		Min	Max	Mean	Std	–
SDM	IJAYA	9.8603E−04	1.0622E−03	9.9204E−04	1.40E−05	397.83
	PGJAYA	**9.8602E−04**	9.8603E−04	**9.8602E−04**	1.45E−09	4.41
	MLBSA	**9.8602E−04**	**9.8602E−04**	**9.8602E−04**	9.15E−12	397.39
	SATLBO	**9.8602E−04**	9.9494E−04	9.8780E−04	2.30E−06	4.95
	GOTLBO	**9.8602E−04**	1.4388E−03	1.0289E−03	1.01E−04	0.88
	TLABC	**9.8602E−04**	1.0397E−03	9.9852E−04	1.86E−05	27.69
	ITLBO	**9.8602E−04**	**9.8602E−04**	**9.8602E−04**	**2.79E−17**	5.95
	JADE	9.8606E−04	1.4103E−03	1.0833E−03	1.09E−04	11.55
	EJADE	**9.8602E−04**	**9.8602E−04**	**9.8602E−04**	**5.13E−17**	11.82
DDM	IJAYA	9.8293E−04	1.4055E−03	1.0269E−03	9.83E−05	393.60
	PGJAYA	9.8263E−04	9.9499E−04	9.8582E−04	2.54E−06	4.95
	MLBSA	9.8249E−04	9.8798E−04	9.8518E−04	1.35E−06	401.25
	SATLBO	9.8280E−04	1.0470E−03	9.9811E−04	1.95E−05	5.70
	GOTLBO	9.8407E−04	1.4380E−03	1.0453E−03	1.01E−04	1.71
	TLABC	9.8415E−04	1.5048E−03	1.0555E−03	1.55E−04	28.01
	ITLBO	**9.8248E−04**	9.8807E−04	9.8448E−04	1.59E−06	6.60
	JADE	9.8351E−04	2.2383E−03	1.4657E−03	3.81E−04	22.29
	EJADE	**9.8248E−04**	**9.8602E−04**	**9.8363E−04**	**1.36E−06**	23.16
Photowatt-PWP201	IJAYA	**2.4251E−03**	2.4393E−03	2.4289E−03	3.78E−06	385.56
	PGJAYA	**2.4251E−03**	2.4268E−03	**2.4251E−03**	3.07E−07	4.46
	MLBSA	**2.4251E−03**	2.4253E−03	**2.4251E−03**	4.34E−08	397.53
	SATLBO	**2.4251E−03**	2.4291E−03	2.4254E−03	7.41E−07	4.87
	GOTLBO	**2.4251E−03**	2.4852E−03	2.4419E−03	1.38E−05	3.51
	TLABC	**2.4251E−03**	2.4458E−03	2.4265E−03	4.00E−06	27.69
	ITLBO	**2.4251E−03**	**2.4251E−03**	**2.4251E−03**	**1.20E−17**	5.83
	JADE	**2.4251E−03**	2.4737E−03	2.4343E−03	1.19E−05	11.49
	EJADE	**2.4251E−03**	**2.4251E−03**	**2.4251E−03**	**3.27E−17**	11.85
STM6-40/36	IJAYA	1.7548E−03	2.5223E−03	1.9305E−03	1.91E−04	350.14
	PGJAYA	**1.7298E−03**	1.7302E−03	**1.7298E−03**	7.82E−08	4.23
	MLBSA	**1.7298E−03**	1.7851E−03	1.7382E−03	1.45E−05	366.53
	SATLBO	**1.7298E−03**	1.7299E−03	**1.7298E−03**	1.22E−08	4.74
	GOTLBO	**1.7298E−03**	1.1244E−02	4.2347E−03	2.68E−03	3.31
	TLABC	**1.7298E−03**	6.5053E−03	2.1827E−03	9.22E−04	27.31
	ITLBO	**1.7298E−03**	**1.7298E−03**	**1.7298E−03**	**7.13E−18**	5.55
	JADE	1.7324E−03	3.2446E−03	2.1308E−03	4.05E−04	16.61
	EJADE	**1.7298E−03**	**1.7298E−03**	**1.7298E−03**	**5.94E−18**	17.01
STP6-120/36	IJAYA	1.6731E−02	1.7304E−02	1.6891E−02	1.12E−04	365.12
	PGJAYA	**1.6601E−02**	1.6611E−02	1.6602E−02	2.57E−06	4.39
	MLBSA	**1.6601E−02**	1.8269E−02	1.6731E−02	3.01E−04	388.09
	SATLBO	**1.6601E−02**	**1.6601E−02**	**1.6601E−02**	2.02E−09	4.98
	GOTLBO	**1.6601E−02**	1.8099E−01	2.9588E−02	3.05E−02	3.48
	TLABC	**1.6601E−02**	2.1497E−02	1.6963E−02	9.47E−04	27.31
	ITLBO	**1.6601E−02**	**1.6601E−02**	**1.6601E−02**	**8.44E−17**	5.79
	JADE	1.7430E−02	3.5903E−02	2.7994E−02	5.62E−03	16.74
	EJADE	**1.6601E−02**	**1.6601E−02**	**1.6601E−02**	**2.33E−17**	17.09

PWP201, while only EJADE and ITLBO are able to achieve the best results for DDM.

- In terms of the Max and Mean RMSE values, it can be obviously seen that EJADE exhibits remarkable performance in comparison algorithms for all models, particularly DDM. Besides, ITLBO, SATLBO, MLBSA, and PGJAYA performed relatively well.
- In regard to Std of RMSE values, it is clear that EJADE and ITLBO have provided the best results, which means that EJADE and ITLBO have a very good robustness. In other words, the parameters extracted by these two algorithms have a good reliability.
- With a view of the CPU time for 30 independent runs, GOTLBO, PGJAYA, SATLBO and ITLBO take the least time, followed by JADE, EJADE, TLABC, IJAYA and MLBSA. Although the shortest time is not obtained by EJADE, it is also considerable compared to TLABC, IJAYA and MLBSA. In addition, it should be pointed out that the calculation of the objective function in this paper is not complicated, the time consumed by the saved *NFE* is not obvious. Once the calculation of the objective function is complicated, other algorithms may consume a large amount of CPU calculation time.

According to the comparison and statistical results, four algorithms, namely ITLBO, SATLBO, MLBSA and PGJAYA, are most competitive to the proposed EJADE algorithm. Hence, more experiments are carried out to further investigate the convergence of these algorithms. For fair comparison, the *Max_NFE* is set to be 50, 000 for all compared algorithms. The convergence curves are given in Fig. 5, where it can be obviously observed that EJADE has the fastest convergence speed for all models, especially for SDM, STM6-40/36 and STP6-120/36 modules. Therefore, it can be concluded that the proposed EJADE algorithm can fast provide an accurate and reliable parameters values compared to other algorithms.

5.5. Discussions of different components

As described in Section 4, in EJADE, there are two improvements that are used to enhance the performance of JADE. In order to analyze

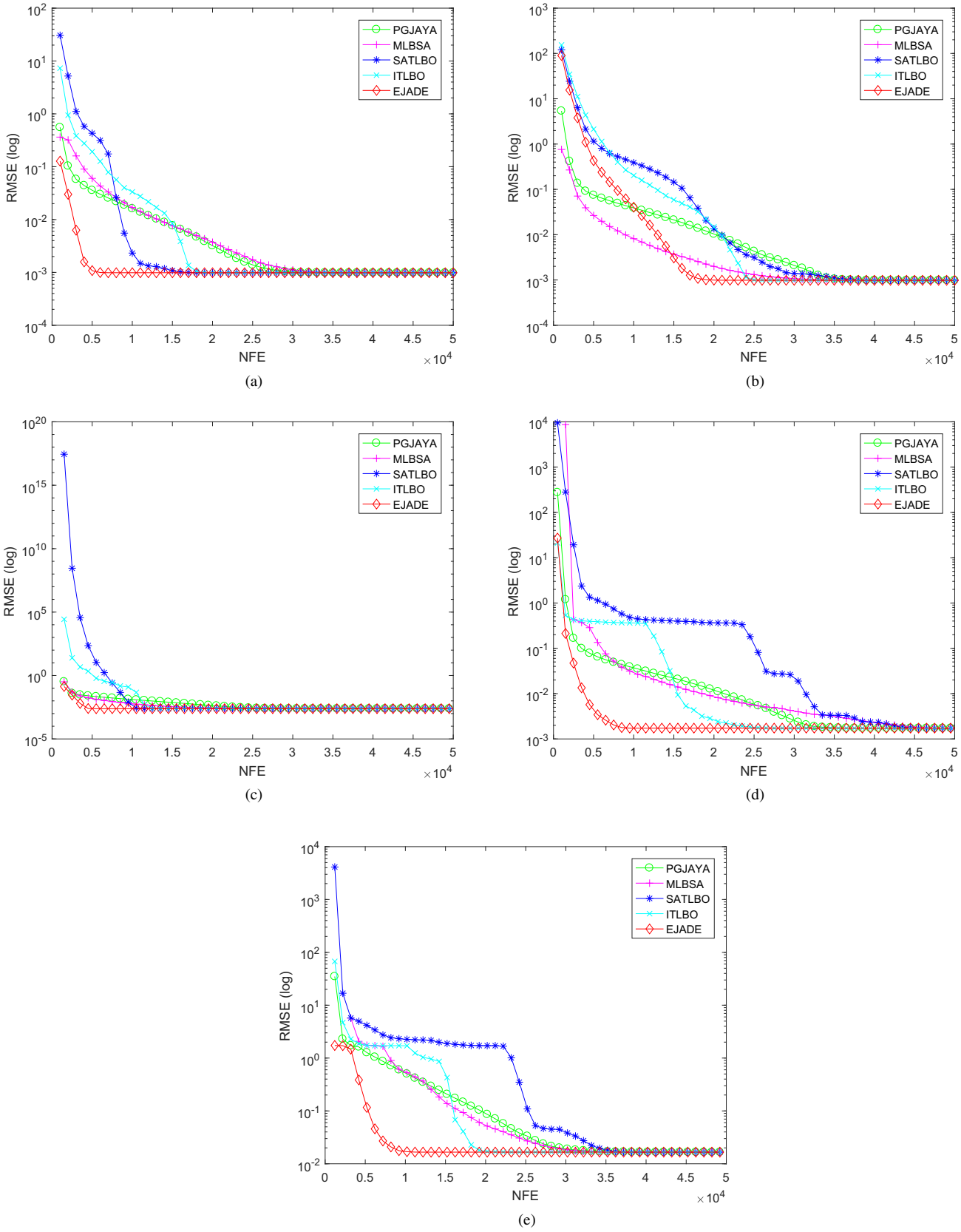

Fig. 5. Convergence curves of different algorithms on PV models: (a) SDM, (b) DDM, (c) Photowatt-PWP201, (d) STM6-40/36, (e) STP6-120/36.

Table 9
Analysis of different components in EJADE for different PV models.

Model	Algorithm	RMSE				CPU time (s)
		Min	Max	Mean	Std	–
SDM	JADE	9.8606E−04	1.4103E−03	1.0833E−03	1.09E−04	11.55
	EJADE−1	**9.8602E−04**	**9.8602E−04**	**9.8602E−04**	3.31E−11	11.63
	EJADE−2	**9.8602E−04**	1.1251E−03	9.9352E−04	2.64E−05	11.91
	EJADE	**9.8602E−04**	**9.8602E−04**	**9.8602E−04**	**5.13E−17**	11.82
DDM	JADE	9.8351E−04	2.2383E−03	1.4657E−03	3.81E−04	22.29
	EJADE−1	**9.8248E−04**	**9.8602E−04**	9.8369E−04	1.26E−06	22.39
	EJADE−2	9.8261E−04	2.0367E−03	1.2866E−03	3.20E−04	22.78
	EJADE	**9.8248E−04**	**9.8602E−04**	**9.8363E−04**	**1.36E−06**	23.16
Photowatt-PWP201	JADE	**2.4251E−03**	2.4737E−03	2.4343E−03	1.19E−05	11.49
	EJADE−1	**2.4251E−03**	**2.4251E−03**	**2.4251E−03**	3.50E−14	11.67
	EJADE−2	**2.4251E−03**	2.4254E−03	**2.4251E−03**	5.11E−08	11.83
	EJADE	**2.4251E−03**	**2.4251E−03**	**2.4251E−03**	**3.27E−17**	11.85
STM6-40/36	JADE	1.7324E−03	3.2446E−03	2.1308E−03	4.05E−04	16.61
	EJADE-1	**1.7298E−03**	**1.7298E−03**	**1.7298E−03**	7.10E−15	16.83
	EJADE−2	**1.7298E−03**	2.7302E−03	1.7657E−03	1.83E−04	17.21
	EJADE	**1.7298E−03**	**1.7298E−03**	**1.7298E−03**	**5.94E−18**	17.01
	JADE	1.7430E−02	3.5903E−02	2.7994E−02	5.62E−03	16.74
STP6-120/36	EJADE-1	**1.6601E−02**	1.6614E−02	**1.6601E−02**	2.85E−06	16.75
	EJADE−2	**1.6601E−02**	3.1945E−02	1.7881E−02	3.56E−03	17.39
	EJADE	**1.6601E−02**	**1.6601E−02**	**1.6601E−02**	**2.33E−17**	17.09

the effectiveness of different components, two EJADE variants are developed, i.e., JADE only with the *CR* sorting mechanism for short as EJADE-1, and JADE only with the dynamic population reduction strategy for short as EJADE-2. The statistical results and convergence curves are reported in Table 9 and Fig. 6, respectively. From the reported results, it can be observed that:

- Compared with JADE, it can be observed that EJADE has a very significant improvement, whether it is minimum, maximum, mean, or standard deviation. In addition, the convergence is also greatly improved.
- For the Min RMSE values, both EJADE-1 and EJADE-2 can provide a better result than original JADE, which indicates that each improvement is very helpful for JADE to find the optimal solution. It is worth mentioning that the introduction of the dynamic population reduction strategy (EJADE-2) can help find optimal solution. The reason may be that it can encourage broader exploration of the search space with a large population size at the early stage while the good solution can be refined with a small population size at the later stage. In addition, for the DDM, EJADE-1 is superior to the EJADE-2.
- With respect to the Max, Mean and Std of RMSE values, EJADE-1 is significantly better than EJADE-2 for all PV models, especially for Mean and Std, which shows that the *CR* sorting mechanism has a good effect on improving the robustness of JADE.
- About the CPU time, it is evident that EJADE adds almost no additional calculation time compared with original JADE.
- Considering the convergence speed, EJADE-2 has a fast convergence rate in the early stage for different models. For SDM and DDM, EJADE-2 is faster than EJADE-1. In contrast, EJADE-1 has better convergence for SMM.
- Taking the comprehensive results into consideration, the proposed EJADE exhibits remarkable performance in terms of accuracy, robustness and convergence.

From the above results and analysis, it can be concluded that the *CR* sorting mechanism plays an important roles in enhancing the accuracy and robustness while the dynamic population reduction strategy will effectively improve the convergence speed. Therefore, it is very necessary to combine the two improvements together to improve the performance of JADE when solving the PV parameter extraction problems.

5.6. Results on experimental data from the manufacturers data sheet

In order to further test the practicality and reliability of the proposed EJADE, two different PV module models (i.e., Multi-crystalline KC200GT [35] and Mono-crystalline SM55 [36]) used in practice are selected as test sets. The experimental data of the two PV module models are obtained by extracting the *I-V* curves given in the manufacturers data sheet at different five irradiance and three temperature conditions. In this section, the above eight well established optimization algorithms are also chosen to compare. For fair comparison, the *Max_NFE* is set to be 30,000 for all compared algorithms. The other parameters are kept same as the corresponding references. In addition, the range of parameters are set as $I_{ph} \in [0, 2I_{SC}]$ (A), $I_o \in [0, 100]$ (μA), $R_s \in [0, 2]$ (Ω), $R_{sh} \in [0, 5000]$ (Ω), and $a \in [1, 4]$. I_{SC} denotes the non-standard conditions short circuit current related to irradiance (G) and temperature (T), which is calculated as follows:

$$I_{SC}(G, T) = I_{SC\_STC} \cdot \frac{G}{G_{STC}} + \alpha \cdot (T - T_{STC}) \tag{29}$$

where I_{SC_STC}, G_{STC}, and T_{STC} represent the short circuit current, irradiance, and temperature at standard test conditions[1], respectively. α is the temperature coefficient for short circuit current at standard test conditions [37].

The statistical results, including the mean and standard deviation of RMSE values for all comparison algorithms are provided in Tables 10–13. It is clear that the proposed EJADE can provide very remarkable and competitive results compared to those state-of-the-art algorithms, regardless of the test conditions of the two PV module models. In addition, to further understand the effects of irradiance and temperature on the extraction parameters, the optimal parameters extracted by EJADE at different irradiance and temperature are reported in Table 14 and Table 15, respectively. Meanwhile, the comparisons between the

[1] Standard test conditions: 1000 W/m^2, 25 °C.

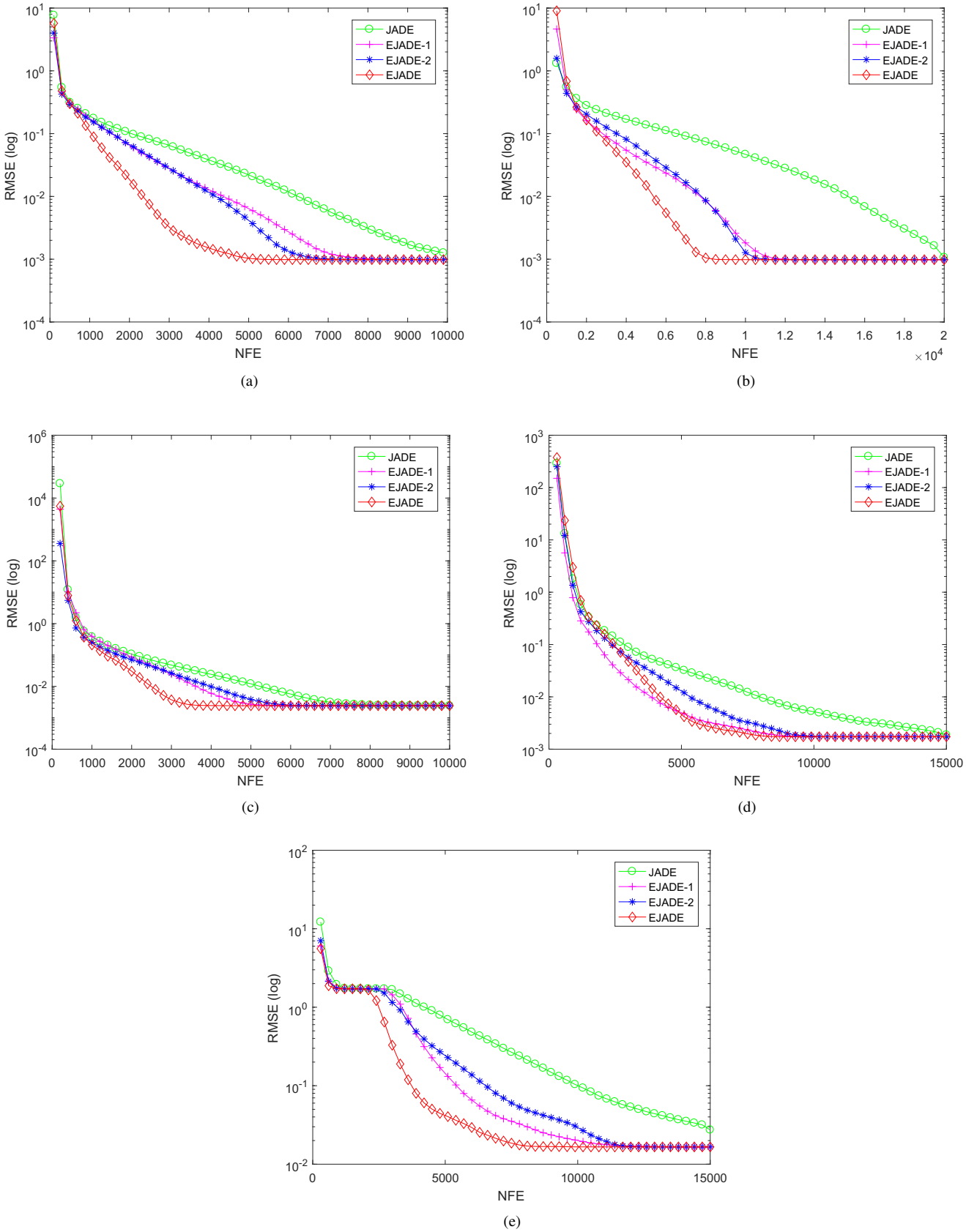

Fig. 6. Convergence curves of different components in EJADE on PV models: (a) SDM, (b) DDM, (c) Photowatt-PWP201, (d) STM6-40/36, (e) STP6-120/36.

Table 10
Results on Multi-crystalline KC200GT PV module at different irradiance and temperature of 25 °C.

Algorithm	200 W/m^2		400 W/m^2		600 W/m^2		800 W/m^2		1000 W/m^2	
	Mean	Std	Mean	Std	Mean	Std	Mean	Std	Mean	Std
IJAYA	4.9949E−03	8.78E−04	9.5808E−03	1.85E−03	2.1362E−02	7.07E−03	4.0320E−02	1.48E−02	4.5729E−02	1.52E−02
PGJAYA	1.5935E−03	1.55E−04	2.3747E−03	4.50E−04	3.7160E−03	1.71E−03	5.5301E−03	1.81E−03	5.8567E−03	1.70E−03
MLBSA	4.2995E−03	2.47E−04	1.0617E−02	1.18E−03	2.2718E−02	2.61E−03	6.7852E−02	1.75E−01	8.1427E−02	2.05E−01
SATLBO	4.0616E−03	9.90E−04	8.0716E−03	1.44E−03	1.1012E−02	2.01E−03	1.8286E−02	3.90E−03	1.7313E−02	3.77E−03
GOTLBO	6.3036E−03	1.58E−03	1.3619E−02	1.83E−03	3.1514E−02	4.44E−03	4.8403E−02	5.29E−03	5.0838E−02	6.70E−03
TLABC	6.0935E−03	1.13E−03	1.3894E−02	1.12E−03	3.2388E−02	3.84E−03	5.1943E−02	5.87E−03	5.7381E−02	6.53E−03
ITLBO	3.5073E−03	9.49E−04	7.1832E−03	1.21E−03	9.8727E−03	1.49E−03	1.5283E−02	1.92E−03	1.4793E−02	3.45E−03
JADE	9.5590E−03	4.59E−03	1.3623E−02	5.43E−03	2.1704E−02	1.67E−02	2.8483E−02	2.59E−02	2.5656E−02	2.91E−02
EJADE	**1.4185E−03**	**1.02E−17**	**1.4262E−03**	**3.95E−17**	**1.2977E−03**	**6.33E−17**	**1.6310E−03**	**1.07E−16**	**1.5390E−03**	**2.11E−16**

Table 11
Results on Multi-crystalline KC200GT PV module at different temperature and irradiance of 1000 W/m^2.

Algorithm	25 °C		50 °C		75 °C	
	Mean	Std	Mean	Std	Mean	Std
IJAYA	4.2041E−02	6.89E−03	2.5492E−02	1.76E−02	8.5805E−03	1.94E−03
PGJAYA	5.8446E−03	1.52E−03	3.6855E−03	8.27E−04	4.6739E−03	1.34E−04
MLBSA	4.1276E−02	8.50E−03	2.5004E−02	1.10E−02	1.0040E−02	3.04E−03
SATLBO	1.7741E−02	6.43E−03	4.7990E−03	1.27E−03	4.5864E−03	1.66E−04
GOTLBO	5.1647E−02	7.34E−03	3.1047E−02	6.99E−03	1.1607E−02	4.15E−03
TLABC	5.6903E−02	7.33E−03	3.5598E−02	6.66E−03	1.5970E−02	6.57E−03
ITLBO	1.5658E−02	4.17E−03	3.7562E−03	8.19E−04	4.4787E−03	2.83E−05
JADE	3.1508E−02	3.16E−02	1.1658E−02	2.01E−02	9.1421E−03	1.04E−02
EJADE	**1.5390E−03**	**2.13E−16**	**2.7465E−03**	**1.96E−16**	**4.4729E−03**	**1.98E−16**

Table 12
Results on Mono-crystalline SM55 PV module at different irradiance and temperature of 25 °C.

Algorithm	200 W/m^2		400 W/m^2		600 W/m^2		800 W/m^2		1000 W/m^2	
	Mean	Std	Mean	Std	Mean	Std	Mean	Std	Mean	Std
IJAYA	8.0179E−04	3.13E−04	2.9197E−03	4.85E−04	7.2602E−03	1.12E−03	7.2725E−03	2.54E−04	8.6061E−03	8.80E−04
PGJAYA	3.2852E−04	1.10E−05	7.5692E−04	6.54E−05	1.1359E−03	2.25E−04	1.3121E−03	5.46E−04	1.9235E−03	6.87E−04
MLBSA	5.3106E−04	7.47E−05	2.6302E−03	4.48E−04	5.6644E−03	1.09E−03	6.4974E−03	1.13E−03	9.2183E−03	1.33E−03
SATLBO	4.2603E−04	9.73E−05	1.4929E−03	3.66E−04	2.2866E−03	8.63E−04	2.6211E−03	1.04E−03	3.0237E−03	1.02E−03
GOTLBO	1.8319E−03	1.76E−03	3.7960E−03	1.30E−03	7.3988E−03	9.85E−04	7.7589E−03	7.31E−04	1.1737E−02	2.59E−03
TLABC	1.3476E−03	8.19E−04	3.0234E−03	2.82E−04	6.8295E−03	9.62E−04	8.0527E−03	9.81E−04	1.3755E−02	2.96E−03
ITLBO	3.4162E−04	3.60E−05	1.1363E−03	3.26E−04	1.8694E−03	7.48E−04	2.5435E−03	1.24E−03	2.7535E−03	1.39E−03
JADE	9.0989E−04	1.26E−03	1.6132E−03	1.32E−03	2.6424E−03	2.70E−03	4.1456E−03	4.19E−03	4.6942E−03	6.50E−03
EJADE	**3.2069E−04**	**3.04E−18**	**7.0761E−04**	**1.02E−17**	**8.2395E−04**	**4.53E−17**	**6.6858E−04**	**4.80E−17**	**1.1462E−03**	**3.97E−17**

Table 13
Results on Mono-crystalline SM55 PV module at different temperature and irradiance of 1000 W/m^2.

Algorithm	25 °C		40 °C		60 °C	
	Mean	Std	Mean	Std	Mean	Std
IJAYA	8.6061E−03	1.46E−03	7.0233E−03	3.55E−04	6.2359E−03	2.69E−04
PGJAYA	1.8798E−03	5.15E−04	4.0030E−03	2.65E−04	3.9754E−03	1.82E−04
MLBSA	9.5951E−03	1.98E−03	6.7112E−03	9.49E−04	5.4580E−03	8.67E−04
SATLBO	2.8433E−03	9.54E−04	3.9161E−03	2.69E−04	3.7841E−03	1.06E−05
GOTLBO	1.2705E−02	3.02E−03	8.1393E−03	1.70E−03	5.4557E−03	8.66E−04
TLABC	1.3059E−02	2.59E−03	8.7236E−03	1.95E−03	5.4291E−03	9.75E−04
ITLBO	2.6784E−03	1.11E−03	3.8054E−03	4.32E−05	3.7851E−03	1.78E−05
JADE	4.7014E−03	6.51E−03	5.8995E−03	4.28E−03	4.6247E−03	1.52E−03
EJADE	**1.1462E−03**	**5.00E−17**	**3.7888E−03**	**1.14E−16**	**3.7804E−03**	**1.50E−16**

Table 14
Optimal parameters extracted by EJADE for two types of PV modules at different irradiance and temperature of 25 °C.

Parameter	Mono-crystalline SM55	Multi-crystalline KC200GT
$G = 200\ W/m^2$		
I_{ph} (A)	0.69150983	1.64615448
I_o (μA)	0.14641172	0.00052100
R_s (Ω)	0.00796166	0.00705762
R_{sh} (Ω)	12.45029748	12.78049260
a	1.38066049	1.00324346
RMSE	3.2069E−04	1.4185E−03
$G = 400\ W/m^2$		
I_{ph} (A)	1.38284413	3.28784893
I_o (μA)	0.10041951	0.00148987
R_s (Ω)	0.01101817	0.00654775
R_{sh} (Ω)	11.86251222	13.92758138
a	1.35198818	1.05503876
RMSE	7.0761E−04	1.4262E−03
$G = 600\ W/m^2$		
I_{ph} (A)	2.07089654	4.93430794
I_o (μA)	0.15551374	0.00386144
R_s (Ω)	0.00918063	0.00624700
R_{sh} (Ω)	12.50190379	13.75928956
a	1.38753423	1.10402054
RMSE	8.2395E−04	1.2977E−03
$G = 800\ W/m^2$		
I_{ph} (A)	2.76038170	6.57132738
I_o (μA)	0.14395059	0.00095306
R_s (Ω)	0.00937751	0.00661732
R_{sh} (Ω)	12.77440241	13.76894813
a	1.38114451	1.03531971
RMSE	6.6858E−04	1.6310E−03
$G = 1000\ W/m^2$		
I_{ph} (A)	3.45010356	8.21689146
I_o (μA)	0.17115392	0.00224195
R_s (Ω)	0.00914299	0.00636693
R_{sh} (Ω)	13.44167955	14.13953974
a	1.39575286	1.07641028
RMSE	1.1462E−03	1.5390E−03

simulated and measured data of the two PV module models at different irradiance and temperature are given in Fig. 7 and Fig. 8, respectively.

From Table 14, it can be obviously observed that for the two PV module models, I_{ph} will be increased while I_o, R_s, R_{sh}, and a have little fluctuation as the irradiance increasing. However, for the temperature effects of the two PV module models, it can be seen that I_{ph} and I_o will be increased while R_s, R_{sh}, and a are kept to be nearly constant as the temperature increasing. In term of the *I-V* curve of the two PV module models shown as Fig. 7 and Fig. 8, it is clear that the simulated and measured data have a good coincidence under different test conditions. It is worth mentioning that EJADE also obtains accurate parameters at low irradiance, which is meaningful for the maximum power point tracking (MPPT) of PV system, because some modules in PV systems are subject to certain mismatch conditions, such as partial shading. In addition, the extracted results can be used in the MPPT model to track the maximum power point, as a varying temperature and radiation in actual applications.

6. Conclusions

Parameter extraction plays an important role in PV systems optimization. In this study, an enhanced adaptive differential evolution algorithm, namely EJADE, has been developed to fast, accurately and reliably extract the unknown parameters of different PV models. In EJADE, the crossover rate sorting mechanism and dynamic population reduction strategy are employed to improve the performance of the JADE algorithm. In order to verify the performance of EJADE, it is used for parameter extraction of different PV models, including the single diode model, the double diode model, and the PV module. The experimental results demonstrate that the proposed EJADE is superior to the original JADE and can fast provide accurate and reliable results compared to those reported in the literature recently. In addition, experiments on two PV module models at different irradiance and temperature also indicate that EJADE has a good practicality, which is helpful for solving the problem of parameter extraction for other complex PV cell models. Therefore, EJADE can be a promising alternative for parameter extraction of PV models. It is worth mentioning that EJADE can not solve the problem of PV models with multiple objective and constraints.

Additionally, the hard condition such as under partial shading of PV system, is not taken into account in this study. So, in the future work, a practical experiment will be carried out by EJADE to solve more complicated PV model parameter extraction problems with these effects into consideration and other energy optimization problems [38], especially for maximum power point tracking (MPPT) problem of PV system.

Table 15
Optimal parameters extracted by EJADE for two types of PV modules at different temperature and irradiance of 1000 W/m^2.

PV module	Temperature	I_{ph} (A)	I_o (μA)	R_s (Ω)	R_{sh} (Ω)	a	RMSE
Mono-crystalline SM55	25 °C	3.45010356	0.17115392	0.00914299	13.44167979	1.39575286	1.1462E−03
	40 °C	3.46913752	1.14510976	0.00869711	14.80747794	1.41783976	3.7888E−03
	60 °C	3.49460847	6.90949935	0.00885294	13.46899847	1.40514174	3.7804E−03
Multi-crystalline KC200GT	25 °C	8.21689146	0.00224195	0.00636693	14.13954085	1.07641029	1.5390E−03
	50 °C	8.29530520	0.12595295	0.00621583	17.66462868	1.11729226	2.7465E−03
	75 °C	8.37766296	1.63082275	0.00634255	14.63996983	1.10147993	4.4729E−03

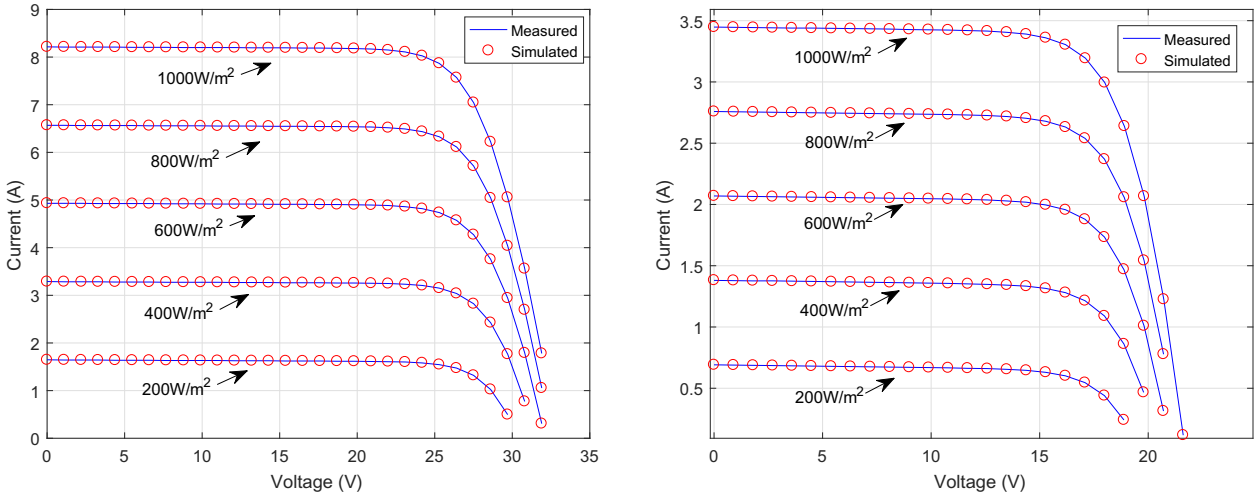

Fig. 7. Comparison between the measured and simulated data obtained by EJADE at different irradiance and temperature of 25 °C: (a) Multi-crystalline KC200GT, (b) Mono-crystalline SM55.

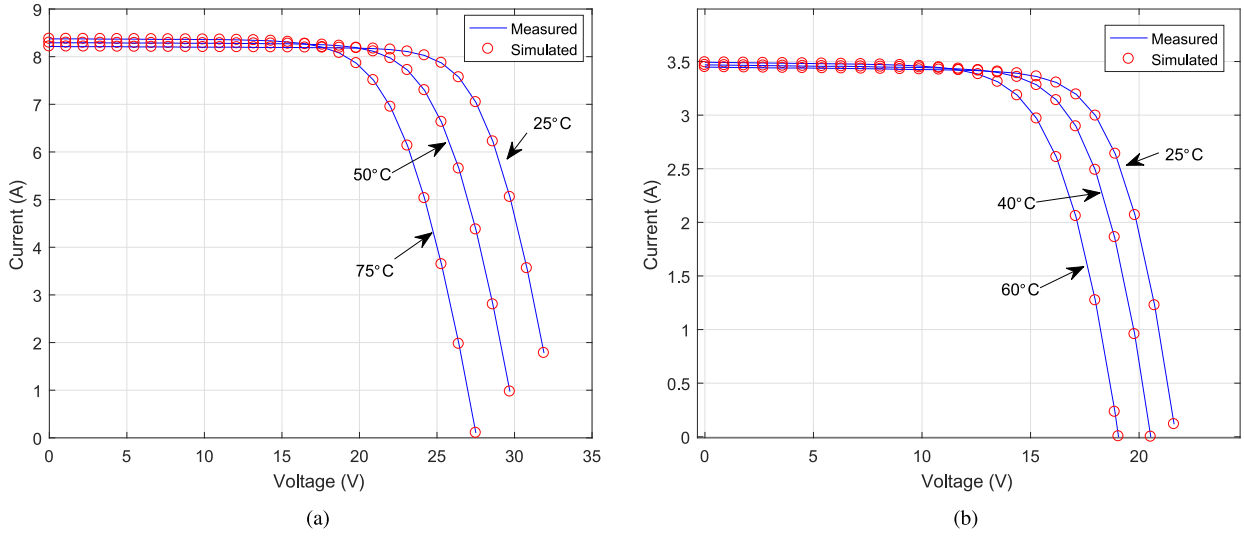

Fig. 8. Comparison between the measured and simulated data obtained by EJADE at different temperature and irradiance of 1000 W/m^2: (a) Multi-crystalline KC200GT, (b) Mono-crystalline SM55.

Declaration of Competing Interest

The authors declare that they have no known competing financial interests or personal relationships that could have appeared to influence the work reported in this paper.

Acknowledgments

This work was partly supported by the National Natural Science Fund of China under Grant Nos. 61573324 and 61873328, the Natural Science Fund for Distinguished Young Scholars of Hubei under Grant No. 2019CFA081, the National Natural Science Fund for Distinguished Young Scholars of China under Grant No. 61525304, the Fundamental Research Funds for the Central Universities, China University of Geosciences (Wuhan) under Grant No. CUGGC03, and the Open Research Fund of the State Key Lab of Digital Manufacturing Equipment & Technology under Grant No. DMETKF2019018.

References

[1] Ayala HVH, dos Santos Coelho L, Mariani VC, Askarzadeh A. An improved free search differential evolution algorithm: a case study on parameters identification of one diode equivalent circuit of a solar cell module. Energy 2015;93:1515–22.
[2] Awadallah MA. Variations of the bacterial foraging algorithm for the extraction of PV module parameters from nameplate data. Energy Convers. Manage. 2016;113:312–20.
[3] Jordehi AR. Parameter estimation of solar photovoltaic (PV) cells: a review. Renew. Sustain. Energy Rev. 2016;61:354–71.
[4] Jordehi AR. Enhanced leader particle swarm optimisation (ELPSO): an efficient algorithm for parameter estimation of photovoltaic (PV) cells and modules. Sol. Energy 2018;159:78–87.
[5] Yeh WC, Huang CL, Lin P, Chen Z, Jiang Y, Sun B. Simplex simplified swarm optimisation for the efficient optimisation of parameter identification for solar cell models. Iet Renewable Power Generation 2018;12(1):45–51.
[6] Parida B, Iniyan S, Goic R. A review of solar photovoltaic technologies. Renewable Sustain. Energy Rev. 2011;15(3):1625–36.
[7] Muhsen DH, Ghazali AB, Khatib T, Abed IA. A comparative study of evolutionary algorithms and adapting control parameters for estimating the parameters of a single-diode photovoltaic module's model. Renewable Energy 2016;96:377–89.
[8] Chin VJ, Salam Z, Ishaque K. Cell modelling and model parameters estimation

techniques for photovoltaic simulator application: a review. Appl. Energy 2015;154:500–19.
[9] Humada AM, Hojabri M, Mekhilef S, Hamada HM. Solar cell parameters extraction based on single and double-diode models: a review. Renew. Sustain. Energy Rev. 2016;56:494–509.
[10] Chen X, Yu K, Du W, Zhao W, Liu G. Parameters identification of solar cell models using generalized oppositional teaching learning based optimization. Energy 2016;99:170–80.
[11] Chan DSH, Phang JCH. Analytical methods for the extraction of solar-cell single- and double-diode model parameters from I-V characteristics. IEEE Trans. Electron Devices 1987;34(2):286–93.
[12] Saleem H, Karmalkar S. An analytical method to extract the physical parameters of a solar cell from four points on the illuminated $j - v$ curve. IEEE Electron Device Lett. 2009;30(4):349–52.
[13] Easwarakhanthan T, Bottin J, Bouhouch I, Boutrit C. Nonlinear minimization algorithm for determining the solar cell parameters with microcomputers. Int. J. Solar Energy 1986;4(1):1–12.
[14] Ortiz-Conde A, Snchez FJG, Muci J. New method to extract the model parameters of solar cells from the explicit analytic solutions of their illuminated characteristics. Solar Energy Mater. Solar Cells 2006;90(3):352–61.
[15] El-Naggar KM, Alrashidi MR, Alhajri MF, Al-Othman AK. Simulated annealing algorithm for photovoltaic parameters identification. Sol. Energy 2012;86(1):266–74.
[16] Zagrouba M, Sellami A, Bouacha M, Ksouri M. Identification of PV solar cells and modules parameters using the genetic algorithms: application to maximum power extraction. Sol. Energy 2010;84(5):860–6.
[17] Merchaoui M, Sakly A, Mimouni MF. Particle swarm optimisation with adaptive mutation strategy for photovoltaic solar cell/module parameter extraction. Energy Convers. Manage. 2018;175:151–63.
[18] Ishaque K, Salam Z, Mekhilef S, Shamsudin A. Parameter extraction of solar photovoltaic modules using penalty-based differential evolution. Appl. Energy 2012;99:297–308.
[19] Gong W, Cai Z. Parameter extraction of solar cell models using repaired adaptive differential evolution. Sol. Energy 2013;94(4):209–20.
[20] Yu K, Liang J, Qu B, Chen X, Wang H. Parameters identification of photovoltaic models using an improved JAYA optimization algorithm. Energy Convers. Manage. 2017;150:742–53.
[21] Yu K, Qu B, Yue C, Ge S, Chen X, Liang J. A performance-guided JAYA algorithm for parameters identification of photovoltaic cell and module. Appl. Energy 2019;237:241–57.
[22] Yu K, Liang JJ, Qu BY, Cheng Z, Wang H. Multiple learning backtracking search algorithm for estimating parameters of photovoltaic models. Appl. Energy 2018;226:408–22.
[23] Yu K, Chen X, Wang X, Wang Z. Parameters identification of photovoltaic models using self-adaptive teaching-learning-based optimization. Energy Convers. Manage. 2017;145:233–46.
[24] Chen X, Xu B, Mei C, Ding Y, Li K. Teaching-learning-based artificial bee colony for solar photovoltaic parameter estimation. Appl. Energy 2018;212:1578–88.
[25] Li S, Gong W, Yan X, Hu C, Bai D, Wang L, Gao L. Parameter extraction of photovoltaic models using an improved teaching-learning-based optimization. Energy Convers. Manage. 2019;186:293–305.
[26] Storn R, Price K. Differential evolution a simple and efficient heuristic for global optimization over continuous spaces. J. Global Optim. 1997;11(4):341–59.
[27] Das S, Mullick SS, Suganthan PN. Recent advances in differential evolution an updated survey. Swarm Evol. Comput. 2016;27:1–30.
[28] Zhang J, Sanderson AC. Jade: adaptive differential evolution with optional external archive. IEEE Trans. Evol. Comput. 2009;13(5):945–58.
[29] Alrashidi MR, Alhajri MF, Elnaggar KM, Alothman AK. A new estimation approach for determining the i–v characteristics of solar cells. Sol. Energy 2011;85(7):1543–50.
[30] Tang L, Yun D, Liu J. Differential evolution with an individual-dependent mechanism. IEEE Trans. Evol. Comput. 2015;19(4):560–74.
[31] Tanabe R, Fukunaga AS. Improving the search performance of shade using linear population size reduction. 2014 IEEE Congress on Evolutionary Computation (CEC). 2014. pp. 1658–1665.
[32] Zhou Y, Yi W, Gao L, Li X. Adaptive differential evolution with sorting crossover rate for continuous optimization problems. IEEE Trans. Cybern. 2017;47(9):2742–53.
[33] Tong NT, Pora W. A parameter extraction technique exploiting intrinsic properties of solar cells. Appl. Energy 2016;176:104–15.
[34] Gao X, Cui Y, Hu J, Xu G, Wang Z, Qu J, Wang H. Parameter extraction of solar cell models using improved shuffled complex evolution algorithm. Energy Convers. Manage. 2018;157:460–79.
[35] KC200GT. High efficiency multicrystal photovoltaic module. URL:https://www.kyocerasolar.com/dealers/product-center/archives/spec-sheets/KC200GT.pdf.
[36] Shell SM55 photovoltaic solar module. URL:https://www.aeet-service.com/pdf/shell/Shell-Solar_SM55.pdf.
[37] Alam D, Yousri D, Eteiba M. Flower pollination algorithm based solar PV parameter estimation. Energy Convers. Manage. 2015;101:410–22.
[38] Ram JP, Babu TS, Rajasekar N. A comprehensive review on solar PV maximum power point tracking techniques. Renew. Sustain. Energy Rev. 2017;67:826–47.